A Unified Approach to RF and Microwave Noise Parameter Modeling in Bipolar Transistors

Guofu Niu, *Member, IEEE*, John D. Cressler, *Fellow, IEEE*, Shiming Zhang, *Student Member, IEEE*, William E. Ansley, Charles S. Webster, and David L. Harame, *Senior Member, IEEE*

***Abstract*—A unified approach to RF and microwave noise parameter modeling in bipolar transistors is presented. Circuit level noise parameters including the minimum noise figure, the optimum generator admittance, and the noise resistance are analytically linked to the fundamental noise sources and the y-parameters of the transistor through circuit analysis of the chain noisy two-port representation. Comparisons of circuit level noise parameters from different physical models of noise sources in the transistor were made against measurements in UHV/CVD SiGe HBTs. A new model for the collector shot noise is then proposed which produces better noise parameter agreement with measured data than the SPICE noise model and the thermodynamic noise model, the two most recent Y-parameter based noise models.**

***Index Terms*—Bipolar technology, chain noisy two-port representation, low noise amplifier (LNA), noise figure, shot noise, SiGe HBT.**

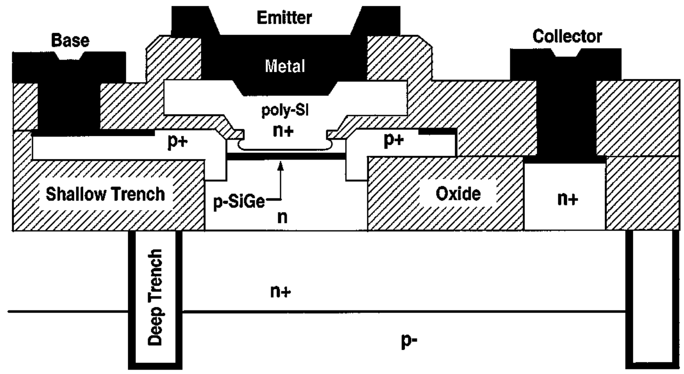

Fig. 1. Schematic cross section of the UHV/CVD SiGe HBT used in this investigation.

I. Introduction

LOW NOISE amplification is an important aspect of transistors at RF and microwave frequencies for applications in the rapidly growing wireless communication market. Models of transistor noise figure were often developed using a small-signal equivalent circuit together with a model for physical noise sources including the shot noise and thermal noise [1]–[4]. Consequently, the expressions obtained for the circuit level noise parameters including the minimum noise figure, the optimum generator admittance, and the noise resistance depend on the specific equivalent circuit employed and the physical noise source model used. Parameter extraction of the equivalent circuit by best-fitting the measured S-parameters often leads to inaccurate noise parameter extraction even from using the same equivalent circuit [5]. The purpose of this work is to develop a unified approach to noise parameter modeling which directly links the circuit level noise parameters to the transistor Y-parameters and the fundamental thermal and shot noise sources. The proposed approach can be easily reduced to recent popular models such as the SPICE noise model [6], and the thermodynamic noise model [7], [8], two of the latest Y-parameter based noise models. Comparisons of circuit level noise parameters from different physical models of noise sources in the transistor [1]–[3], [6], [7] are then made against measurements of UHV/CVD SiGe HBTs [9], [10]. Unphysical results were obtained when several existing models for the collector and base shot noise correlation were used. A new collector shot noise model is proposed to better model the measured noise parameters.

Manuscript received June 25, 1999; revised February 25, 2001. This work was supported by IBM under an IBM University Partnership Research Program Award, and Semiconductor Research Corporation under SRC 2000-HJ-769. The review of this paper was arranged by Editors P. Asbeck and T. Nakamura.

G. Niu, J. D. Cressler, and S. Zhang are with the Alabama Microelectronics Science and Technology Center, Electrical Engineering Department, Auburn University, Auburn, AL 36849 USA (e-mail: guofu@eng.auburn.edu).

W. E. Ansley is with IBM Microelectronics, Hopewell Junction, NY 12533 USA.

C. S. Webster and D. L. Harame are with IBM Microelectronics, Essex Junction, VT 05452 USA.

Publisher Item Identifier S 0018-9383(01)09069-4.

II. Device Technology and Measurement Setup

The SiGe HBTs used in this work were fabricated using a self-aligned, epitaxial-base technology [9], [10]. Fig. 1 shows a schematic cross section of the device. The SiGe base is formed in an ultrahigh-vacuum/chemical vapor deposition (UHV/CVD) low temperature epitaxy (LTE) system. Polysilicon deposited over the field oxide during the LTE growth serves as the extrinsic base contact. Polysilicon-filled, closed-bottom, deep trenches isolate adjacent sub-collectors, and the field oxide is fabricated using a planar shallow trench process. The intrinsic collector was formed by a double implantation to realize high performance. Representative vertical doping and Ge profiles of the standard SiGe HBT are shown in Fig. 2. DC characteristics were measured on-wafer using an HP4155, and ac characteristics were measured on-wafer using an HP8510C network analyzer. The noise parameters of a $0.5 \times 20 \times 2\ \mu\mathrm{m}^2$ standard device were measured from 2–18 GHz using an NP-5 on-wafer measurement system from ATN Microwave, Inc.

III. The Unified Noise Modeling Approach

Circuit theory shows that any noisy linear network can be replaced by its noiseless counterpart, an input-referred current noise generator i_n, an input-referred voltage noise generator v_n,

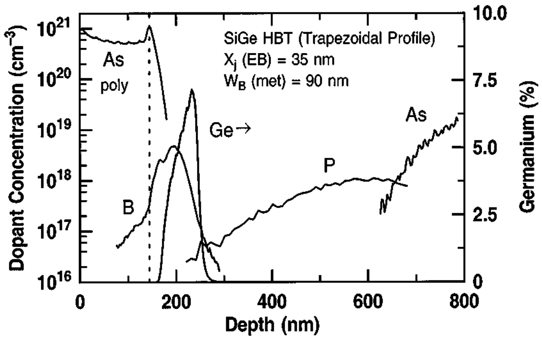

Fig. 2. Representative SIMS doping and Ge profiles of the UHV/CVD SiGe HBTs.

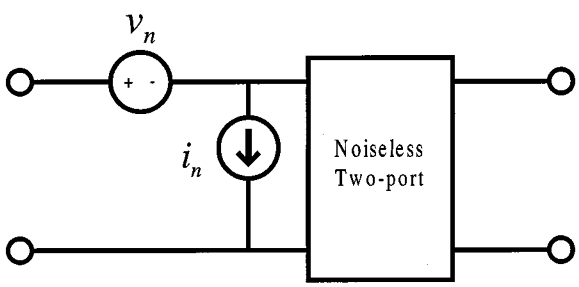

Fig. 3. Schematic of the chain noisy two-port representation for a linear noisy two-port.

and their cross-correlation $\langle v_n i_n^* \rangle$ [11], as shown in Fig. 3. It is worth noting that the polarity arrangement of the voltage noise source and the current noise source is important because they are in general correlated to each other. Independent of the physical sources of noise inside the device, the four circuit level noise parameters, including the minimum noise factor $F_{\min}$, the real and imaginary parts of the optimum generator admittance $Y_{opt} = G_{G,\,opt} + jB_{G,\,opt}$, and the noise resistance R_n, can be expressed as a function of $\langle i_n^2 \rangle$, $\langle v_n^2 \rangle$, and $\langle v_n i_n^* \rangle$ [11]–[13]

$$F_{\min} = 1 + 2\left(C_r + \sqrt{R_n G_n - C_i^2}\right) \tag{1}$$

$$G_{G,\,opt} = \sqrt{\frac{G_n}{R_n} - \left(\frac{C_i}{R_n}\right)^2} \tag{2}$$

$$B_{G,\,opt} = \frac{C_i}{R_n} \tag{3}$$

$$R_n = \frac{\langle v_n^2 \rangle}{4kT\,\Delta f} \tag{4}$$

where

$$G_n = \frac{\langle i_n^2 \rangle}{4kT\,\Delta f} \tag{5}$$

$$C_r = \frac{\mathrm{Re}\,\{\langle v_n i_n^* \rangle\}}{4kT\,\Delta f} \tag{6}$$

$$C_i = \frac{\mathrm{Im}\,\{\langle v_n i_n^* \rangle\}}{4kT\,\Delta f}. \tag{7}$$

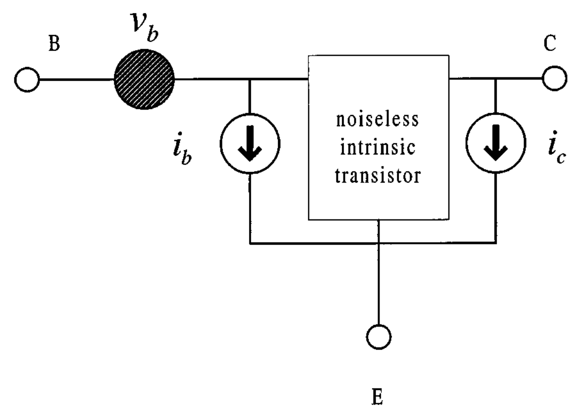

Fig. 4. Representation of the noise sources in a bipolar transistor for the common-emitter configuration used in this work.

The noise factor for any arbitrary generator admittance $Y_G = G_G + jB_G$ is given by [11]

$$F = F_{\min} + \frac{R_n}{G_G}\,|Y_G - Y_{G,\,opt}|^2. \tag{8}$$

Equation (8) forms the basis of noise factor measurement and is widely used in circuit design. The reflection coefficient $\Gamma_{\mathrm{G,\,opt}}$, instead of the admittance $\mathrm{Y_{G,\,opt}}$ is often used in noise measurements

$$\Gamma_{G,\,opt} = \frac{1 - Y_{G,\,opt} Z_0}{1 + Y_{G,\,opt} Z_0} \tag{9}$$

where $\mathrm{Z_0}$ is the characteristic impedance and is equal to 50 Ω here.

At RF and microwave frequencies, the dominant noise sources are the base resistance-induced thermal noise, and the terminal current shot noises. Fig. 4 shows a representation of these noise sources for the common emitter configuration used in this work. Note that the base current shot noise is directly tied between the emitter and the base, as opposed to between the emitter and an internal base node connected to the base through the base resistance [1]–[6]. Strictly speaking, the distributive nature of base current flow requires a distributive description of the associated shot noise, or a split of the total base current shot noise between the internal base node and the external base node. In real devices, however, such a separation makes little difference at frequencies below the cut-off frequency, because the base resistance is far smaller than both the transistor input impedance and the optimum source impedance for minimum noise figure. Connecting the base shot noise i_b directly between the external base and the emitter considerably simplifies analytical noise analysis, and allows direct modeling of noise from measured S-parameters, as detailed below. The $f < f_T$ assumption used in [6] to simplify the noise figure equation is indeed equivalent to connecting i_b directly between the external base and the emitter.

The base and collector shot noises i_b and i_c are in general correlated to each other. The polarity of the base thermal noise v_b is not important here because it is independent of the shot noises. The relative polarity arrangement of i_b and i_c are important when they are correlated. We choose here the common-emitter

TABLE I
COMPARISON OF THE FUNDAMENTAL NOISE SOURCES BETWEEN THE THERMODYNAMIC NOISE MODEL AND THE SPICE NOISE MODEL. THE SUPERSCRIPT $*$ STANDS FOR THE CONJUGATE

	Thermodynamic Model	SPICE Model
$<v_b^2>$	0	$4kTr_B$
$<i_b^2>$	$4kTRe\{Y_{11}\} + 2qI_B$	$2qI_B$
$<i_c^2>$	$2qI_C$	$2qI_C$
$<i_c i_b^*>$	0	0

configuration, which gives better stability over a wide range of operating conditions. Next, we transform the transistor noise representation in Fig. 4 into the chain noisy two-port representation in Fig. 3 by circuit analysis

$$\langle v_n^2\rangle = \frac{\langle i_c^2\rangle}{|Y_{21}|^2} + \langle v_b^2\rangle \tag{10}$$

$$\langle i_n^2\rangle = \langle i_b^2\rangle + \frac{\langle i_c^2\rangle}{|h_{21}|^2} - 2\mathrm{Re}\left(\frac{\langle i_b^* i_c\rangle}{h_{21}}\right) \tag{11}$$

$$\langle v_n i_n^*\rangle = \frac{\langle i_c^2\rangle}{|Y_{21}|^2} Y_{11}^* - \frac{\langle i_b^* i_c\rangle}{Y_{21}} \tag{12}$$

where $h_{21} = Y_{21}/Y_{11}$ by definition. Given a model for the base and collector shot noise, all of the noise parameters can be readily obtained by substituting (10)–(12) into (1)–(7). For instance, the SPICE noise model, originally derived in [6], is readily obtained by setting the base and collector shot noise to $2\mathrm{qI_B}$ and $2\mathrm{qI_C}$, respectively, and setting their cross-correlation to zero. The thermodynamic noise model [7], [8], which describes the thermal noise through an input current noise source $4\mathrm{kTRe}\{\mathrm{Y}_{11}\}$, can also be obtained by proper setting of the base and collector noise currents. A comparison of the two popular noise models in terms of the fundamental noise sources is given in Table I [14]. The results of noise parameters obtained using the unified approach are verified to be identical to those originally derived in [6] and [7].

Several other noise models such as the Nielson's [1] and Hawkins's [2] models were derived using the common-base configuration. In these models, the noise sources associated with the collector and emitter currents were used. Common-base noise sources can be easily converted to common-emitter noise sources by equivalent circuit analysis

$$\langle i_b^2\rangle = \langle i_e^2\rangle + \langle i_c^2\rangle - 2\mathrm{Re}\left\{\langle i_c i_e^*\rangle\right\} \tag{13}$$

$$\langle i_b^* i_c\rangle = \langle i_c i_e^*\rangle - \langle i_c^2\rangle \tag{14}$$

where Re refers to taking the real part of the argument. In Nielson's model, both the emitter and collector currents contain shot noise, and the emitter shot noise transports to the collector in the same way as the signal, leading to a cross-correlation through the small signal gain

$$\langle i_e^2\rangle = 2qI_E \tag{15}$$

$$\langle i_c^2\rangle = 2qI_C \tag{16}$$

$$\langle i_e i_c^*\rangle = \alpha_{AC}\langle i_e^2\rangle = \alpha_{AC} 2qI_E. \tag{17}$$

The part of the collector–base junction shot noise i_c that is not correlated to the emitter–base junction shot noise i_e is often referred to as the collector partition noise i_{cp} [1]. The expressions for the common-emitter version of shot noise representation can be obtained by substituting (15)–(17) into (13) and (14). Compared to the shot noise model in SPICE, the base shot noise is no longer $2qI_B$, and the cross-correlation between i_b and i_c is no longer zero in general. Equations (15)–(17) can be formally reduced to the SPICE shot noise model by replacing the common-base small-signal current gain with the common-base DC current gain, which leads to $\langle i_e i_c^*\rangle = \alpha_{DC} 2qI_E = 2qI_C$, $\langle i_b^2\rangle = 2qI_B$, and $\langle i_b i_c^*\rangle = 0$. Hawkins's model accounted for the emitter–base depletion capacitance and replaced the small signal current gain in (17) with the small signal base transport factor [2]. The equivalent circuit Hawkins's used, however, is a simplified one, and does not account for the emitter–base junction diffusion capacitance for the input circuit. Another model for the correlation of the emitter and collector shot noises is van der Zeil's model [3], which takes into account the high frequency conductance change. Again, the noise was expected to behave in the same way as the signal in his theory for the cross-correlation between emitter and collector shot noises.

Next we measured the S-parameters of UHV/CVD SiGe HBTs and extracted the base resistance using the impedance circle method [15]. Different noise source models were then substituted into the general modeling equations relating the fundamental noise sources to the four noise parameters. For the three shot noise models with correlation between the base and collector shot noise, namely the Nielson's [1], Hawkins's [2], and van der Zeil's model [3], negative numbers (unphysical) were obtained for the square root functions in (1) and (2), the general purpose noise parameter equation for noisy two-ports. In contrast, such negative numbers were never observed for the SPICE noise model and the thermodynamic noise model. Because both $\langle i_e^2\rangle = 2qI_E$ and $\langle i_c^2\rangle = 2qI_C$ are pre-determined as shot noise, the unphysical results can only be corrected through the modification of the cross-correlation $\langle i_e i_c^*\rangle$. A step-by-step examination of the numerical procedure indeed shows that the cross-correlation term $\langle i_e i_c^*\rangle$ is responsible for the negative numbers observed, suggesting that previous approaches to the cross-correlation are in error. As mentioned earlier, setting $\langle i_e i_c^*\rangle = 2qI_C$ reduces the Nielson's model to the SPICE noise model. We propose in the following a new physical mechanism for the collector shot noise which leads to a new model for the cross-correlation term $\langle i_e i_c^*\rangle$. The new model avoids the negative number problem, and allows a better fitting of the measured noise parameters than the SPICE noise model and the thermodynamic noise model.

IV. A NEW COLLECTOR SHOT NOISE MODEL

The essence of the conventional shot noise theory in junction transistors is that any dc current passing through a pn junction shows full shot noise. The collector current noise is therefore always $2\mathrm{qI_C}$ independent of what comes into the collector–base junction. The emitter current shot noise transports to the collector-base junction in the same way as the signal, and the same carriers that arrive at the collector-base junction contribute to

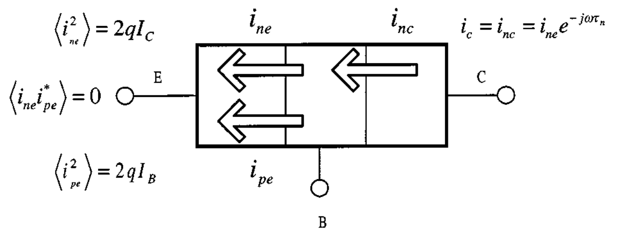

Fig. 5. Illustration of the new shot noise model for a bipolar transistor. The collector shot noise is fully attributed to and thus completely correlated to the shot noise associated with the electron injection from the emitter.

the $2\mathrm{qI_C}$ shot noise, leading to the cross-correlation $\langle i_e i_c^* \rangle = \alpha_{AC} \langle i_e^2 \rangle = \alpha_{AC} 2qI_E$ in (17). We question here the validity of the above physical mechanism for the collector shot noise. The concept of shot noise originated from the random noise in a vacuum thermonic diode. In analogy, the transition of carriers across a pn junction through diffusion is also a random event depending on the carriers having sufficient energy to overcome the potential barrier. Each event causes a random current pulse to occur at the external terminal. The transition of carriers across the collector–base junction, which is usually *reverse-biased* for low noise amplification, however, is a *drift* process, and therefore a dc current passing through such a junction alone does not have intrinsic shot noise. The collector current shows shot noise only because the electron current being injected into the collector–base junction from the emitter already has shot noise, as shown in Fig. 5. The emitter current shot noise consists of two parts, $\langle i_{ne}^2 \rangle = 2qI_C$, due to the electron injection into the base, and $\langle i_{pe}^2 \rangle = 2qI_B$, due to the hole injection into the emitter. These processes are independent of each other because the electron and hole injections are independent. The collector current shot noise is therefore physically a delayed version of the emitter electron injection induced shot noise, $i_c = i_{nc} = i_{ne} e^{-j\omega\tau_n}$, where τ_n is the transit time associated with the transport of emitter-injected electron shot noise current, and includes both the transit time in the base and the transit time in the collector–base junction. In contrast to previous theory, the collector shot noise is fully attributed to the transport from the emitter with a frequency dependent phase delay characterized by a time constant, as opposed to the inherent shot noise associated with the collector–base junction. We are opposed to the concept that the high frequency noise transports in the same way as the signal, which underlies $\langle i_e i_c^* \rangle = \alpha_{AC} \langle i_e^2 \rangle = \alpha_{AC} 2qI_E$ in (17), because of the following.

1) The high frequency signal current involves the charging of depletion and diffusion capacitances through the movement of both electrons and holes, and the signal current diminishes when reaching the collector at very high frequencies.
2) The electron shot noise current due to the random nature of crossing the emitter–base junction barrier does not involve the above capacitance charging processes.
3) The $2qI_C$ shot noise level which is often measured at the collector has to come from the shot noise intrinsic to the electrons injected to the collector–base junction, since a dc drift current passing through a reverse-biased junction does not show shot noise.
4) The $2qI_C$ shot noise measured at the collector, therefore, must have come from the emitter without any magnitude degradation.

Consequently, we propose the common-base version of the new shot noise model

$$\langle i_c^2 \rangle = \langle i_{nc} i_{nc}^* \rangle = 2qI_C \tag{18}$$

$$\langle i_e^2 \rangle = \langle i_{ne}^2 \rangle + \langle i_{pe}^2 \rangle = 2qI_E \tag{19}$$

$$\langle i_e i_c^* \rangle = 2qI_C e^{j\omega\tau_n}. \tag{20}$$

The collector shot noise is solely determined and thus *fully* correlated to the electron current noise coming from the emitter with a frequency dependent phase delay. A large built-in electric field due to Ge grading in the base helps reducing the base transit time, and hence τ_n, which may enhance the correlation between the emitter and collector shot noise. Equations (18)–(20) can be converted to the common-emitter version using (13)–(14)

$$\begin{aligned}\langle i_b^2 \rangle &= \langle i_e^2 \rangle + \langle i_c^2 \rangle - 2\mathrm{Re}\left\{\langle i_e i_c^* \rangle\right\} \\ &= 2qI_E + 2qI_C - 4qI_C \mathrm{Re}\left\{e^{j\omega\tau_n}\right\}\end{aligned} \tag{21}$$

$$\langle i_c^2 \rangle = 2qI_C \tag{22}$$

$$\begin{aligned}\langle i_b^* i_c \rangle &= \left\{\langle i_e i_c^* \rangle\right\}^* - \langle i_c^2 \rangle \\ &= 2qI_C e^{-j\omega\tau_n} - 2qI_C.\end{aligned} \tag{23}$$

Setting the noise transit time parameter to zero reduces the new shot noise model to the shot noise model used in the SPICE noise model [6].

V. Experiments and Model Verification

For verification, the new shot noise model is applied to reproduce the measured noise parameters of a typical UHV/CVD SiGe HBT with an emitter size of 0.5 (emitter width) $\times$ 20 (emitter length) $\times$ 2 (number of emitter fingers) $\mu\mathrm{m}^2$. As can be seen from (20), the noise transit time parameter characterizes the frequency dependence of the cross-correlation, and is therefore expected to produce certain frequency dependence of noise figure that is different from the conventional SPICE noise model. We can therefore extract the noise transit time by fitting the measured frequency dependence of noise figure. A good fitting of the frequency dependence of noise figure, indeed, can be achieved using a cross-correlation with the functional form of (20), as described later. For a complete discussion, we examine both the frequency and current dependence of all of the three noise parameters including the minimum noise factor $\mathrm{F_{min}}$ [through the minimum noise figure $\mathrm{NF_{min}} = 10\log(\mathrm{F_{min}})$], the optimum admittance $\mathrm{Y_{G,\,opt}}$ (through $\Gamma_{\mathrm{G,\,opt}}$), and the noise resistance $\mathrm{R_n}$.

A. Minimum Noise Factor $F_{\min}$ (Through Minimum Noise Figure $\mathrm{NF_{min}} = 10\log \mathrm{F_{min}}$)

First, the S-parameters were measured and converted to Y-parameters, which were subsequently used in (10)–(12). The base resistance was determined from the left intercept of the

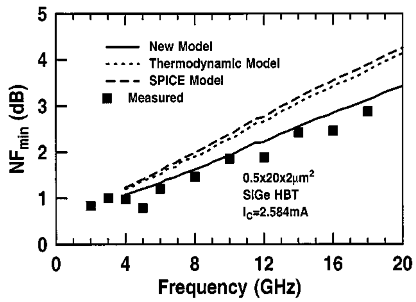

Fig. 6. Comparison of modeled and measured $\mathrm{NF}_{\min}$ versus frequency ($\mathrm{I_C} = 2.584$ mA and $\mathrm{A_E} = 0.5 \times 20 \times 2 \mu\mathrm{m}^2$).

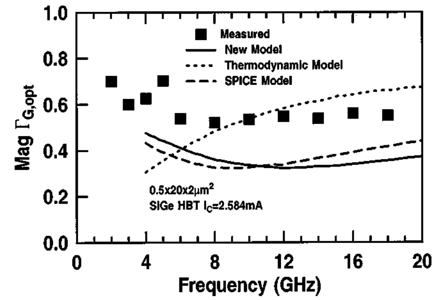

Fig. 8. Comparison of modeled and measured magnitude of $\Gamma_{G,opt}$ versus frequency at $\mathrm{I_C} = 2.584$ mA.

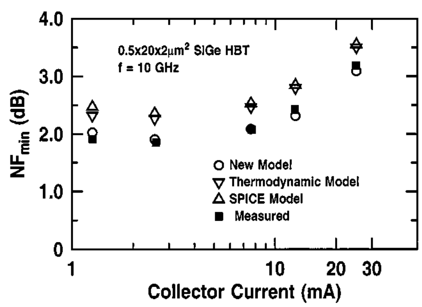

Fig. 7. Comparison of modeled and measured $\mathrm{NF}_{\min}$ versus current at 10 GHz.

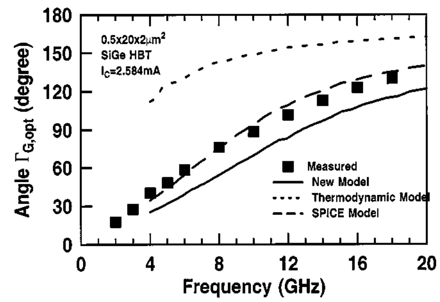

Fig. 9. Comparison of modeled and measured angle of $\Gamma_{G,opt}$ versus frequency at $\mathrm{I_C} = 2.584$ mA.

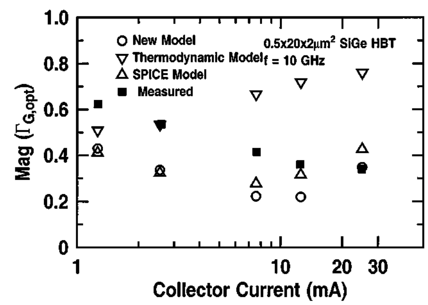

Fig. 10. Comparison of modeled and measured magnitude of $\Gamma_{G,opt}$ versus current at 10 GHz.

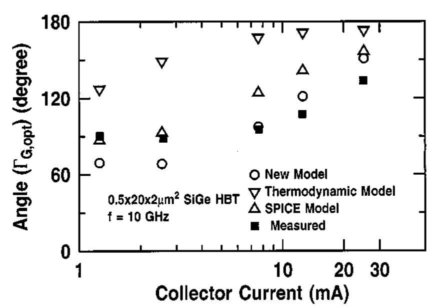

Fig. 11. Comparison of modeled and measured angle of $\Gamma_{G,opt}$ versus current at 10 GHz.

semi-circle on the complex plane of the input impedance [13]. Fig. 6 shows the measured and modeled minimum noise figure ($\mathrm{NF_{min}} = 10 \log \mathrm{F_{min}}$) versus frequency at 2.584 mA. As mentioned earlier, the Nielson's, Hawkins's, and Van der Zeil's models with a frequency dependent $\langle i_e i_c^* \rangle$ produced negative numbers for the square root functions in the general purpose noise parameter equations, and thus cannot be shown here. The other two popular models, namely the SPICE noise model, and the thermodynamic noise model, were found to overestimate the noise figure at higher frequencies, as can be seen from Fig. 6. The new shot noise model, characterized by a frequency dependent cross-correlation with the functional form of (20), produces a better agreement to the measured data. A value of 1.5 ps was extracted for the noise transit time by best-fitting the minimum noise figure versus frequency curve, which is in the same order of magnitude as the transit time τ_{ec} extracted from the $1/f_{\mathrm{T}}$ versus $1/I_{\mathrm{C}}$ curve (3.1 ps). A good initial guess for the noise transit time is zero, which corresponds to the SPICE noise model. τ_{ec} extracted from the $1/\mathrm{f_T}$ versus $1/\mathrm{I_C}$ curve can be used as a reference for the extraction of the noise transit time. A systematic experimental investigation on more hardware is needed in future work to explore the relation between the noise transit time and other transistor parameters such as the base and collector transit times. The new shot noise model works well at higher currents. Fig. 7 shows the current dependence of $\mathrm{NF_{min}}$ at 10 GHz.

B. Optimum Generator Admittance $Y_{G,opt}$ ($\Gamma_{G,opt}$)

The other important noise parameter is the optimum generator admittance $Y_{G,opt}$, which is often characterized by the reflection coefficient at minimum noise figure ($\Gamma_{G,opt}$) in measurement. Figs. 8 and 9 show the magnitude and angle of $\Gamma_{G,opt}$ [defined in (9)] versus frequency at 2.584 mA, and Figs. 10 and 11 show the magnitude and angle of $\Gamma_{G,opt}$ versus current at 10 GHz. From a measurement standpoint, the accuracy of the minimum noise figure is the highest among all of the three measured noise parameters. Therefore, we extracted the noise transit

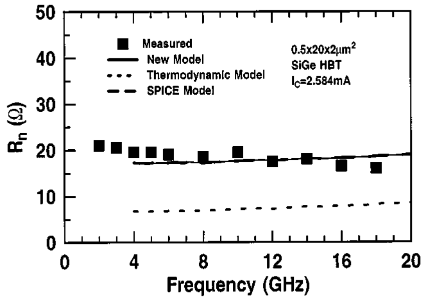

Fig. 12. Comparison of modeled and measured R_n versus frequency at $\mathrm{I_C} = 2.584$ mA.

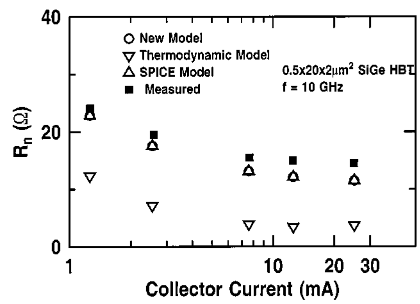

Fig. 13. Comparison of modeled and measured R_n versus current at 10 GHz.

time model parameter by best fitting the minimum noise figure, rather than $Y_{G,\,opt}$.

C. Noise Resistance R_n

The associated gain of a device at minimum noise figure may not be sufficient for applications such as a low noise amplifier. In this situation, a compromise between input matching for minimum noise figure and power gain can be made. The noise resistance, $\mathrm{R_n}$, determines the sensitivity of the total noise figure to deviations from optimum noise admittance matching $\mathrm{Y_{G,\,opt}}$, as can be seen from (8). Figs. 12 and 13 show the frequency and current dependence of $\mathrm{R_n}$. According to the linear two-port noise theory, $\mathrm{R_n}$ is determined by the input-referred noise voltage $\langle v_n^2 \rangle$ [see (4)]. $\langle v_n^2 \rangle$ is determined by the collector shot noise and the base thermal noise, which are the same for the proposed model and the SPICE noise model, despite the very different physical mechanisms for the collector shot noise. Consequently the new shot noise model and the SPICE noise model produce the same $\mathrm{R_n}$. The thermodynamic noise model describes the thermal noise through an input current noise, instead of a base resistance, thus producing a smaller $\langle v_n^2 \rangle$ and a smaller $\mathrm{R_n}$. The description of thermal noise through base resistance, however, produces a close agreement with the measured $\mathrm{R_n}$ in the SiGe HBTs under study.

VI. Conclusions

We have presented a unified noise modeling approach which links the fundamental noise current sources to the circuit level noise parameters including the minimum noise figure, the optimum admittance, and the noise resistance. The new approach makes easier the comparison of the impacts of different physical noise source models on circuit level noise parameters that can be measured experimentally. Experiments on UHV/CVD SiGe HBTs produces unphysical results for several existing noise source models, and the cross-correlation between the emitter and collector was identified to be the problem. A new model for the collector shot-noise, which attributes the $2q\mathrm{I_C}$ collector shot noise fully to the transport from the emitter, is proposed and verified to produce better agreement to measurement than popular models such as the SPICE noise model and the thermodynamic noise model.

Acknowledgment

The authors would like to thank D. Ahlgren, D. Harame, S. Subbanna, J. Moniz, A. J. Joseph, B. Meyerson, U. Gogineni, and S. Mathew for their support of this work, and R. Plana, for providing the derivations of the noise equations in [12].

References

[1] E. C. Neilsen, "Behavior of noise figure in junction transistors," *Proc. IRE*, vol. 45, pp. 957–963, July 1957.

[2] R. J. Hawkins, "Limitations of Nielson's and related noise equations applied to microwave bipolar transistors, and a new expression for the frequency and current dependent noise figure," *Solid-State Electron.*, vol. 20, pp. 191–196, 1977.

[3] G. H. Hanson and A. van der Ziel, "Shot noise in transistors," *Proc. IRE*, vol. 45, pp. 1538–1542, Nov. 1957.

[4] H. Fukui, "The noise performance of microwave transistors," *IEEE Trans. Electron Devices*, vol. ED-13, pp. 329–341, Mar. 1966.

[5] J. P. Roux, L. Escotte, R. Planna, J. Graffeuil, S. L. Delage, and H. Blanck, "Small-signal and noise model extraction technique for heterojunction bipolar transistors at microwave frequencies," *IEEE Trans. Electron Devices*, vol. 43, pp. 293–297, Feb. 1995.

[6] S. P. Voinigescu, M. C. Maliepaard, J. L. Showell, G. E. Babcock, D. Marchesan, M. Schroter, P. Schvan, and D. L. Harame, "A scalable high-frequency noise model for bipolar transistors with application to optimal transistor sizing for low-noise amplifier design," *IEEE J. Solid-State Circuits*, vol. 32, pp. 1430–1438, Sept. 1997.

[7] F. Herzel and B. Heinemann, "High frequency noise of bipolar devices in consideration of carrier heating and low temperature effects," *Solid-State Electron.*, vol. 38, pp. 1905–1909, Nov. 1995.

[8] F. Herzel, P. Schley, B. Heinemann, U. Zilmann, D. Knoll, D. Temmler, and U. Erben, "Experimental verification and numerical application of the thermodynamic approach to high frequency noise in SiGe HBTs," *Solid-State Electron.*, vol. 41, pp. 387–390, March 1997.

[9] D. L. Harame, J. H. Comfort, J. D. Cressler, E. F. Crabbé, J. Y. C. Sun, B. S. Meyerson, and T. Tice, "Si/SiGe epitaxial-base transistors—Part I: Materials, physics, and circuits," *IEEE Trans. Electron Devices*, vol. 42, pp. 469–482, Mar. 1995.

[10] D. C. Ahlgren, G. Freeman, S. Subbanna, R. Groves, D. Greenberg, J. Malinowski, D. Nguyen-Ngoc, S. J. Jeng, K. Stein, K. Schonenberg, D. Kiesling, B. Martin, S. Wu, D. L. Harame, and B. Meyerson, "A SiGe HBT BiCMOS technology for mixed signal RF applications," in *Proc. IEEE BCTM*, Sept. 1997, pp. 195–198.

[11] H. A. Haus, W. R. Atkinson, W. H. Fonger, W. W. Mcleod, G. M. Branch, W. A. Harris, E. K. Stodola, W. B. Davenport, Jr., S. W. Harrison, and T. E. Talpey, "Representation of noise in linear twoports," *Proc. IRE*, vol. 48, pp. 69–74, Jan. 1960.

[12] L. Escotte, J. Roux, R. Plana, J. Graffeuil, and A. Gruhle, "Noise modeling of microwave heterojunction bipolar transistors," *IEEE Trans. Electron Devices*, vol. 42, pp. 883–888, May 1995.

[13] H. Hillbrand and P. H. Russer, "An efficient method for computer aided noise analysis of linear amplifier networks," *IEEE Trans. Circuits Syst.*, vol. CAS-23, pp. 235–238, Apr. 1976.

[14] G. Niu, W. Ansley, S. Zhang, J. D. Cressler, C. S. Webster, and R. A. Groves, "Noise parameter optimization of UHV/CVD SiGe HBTs for RF and microwave applications," *IEEE Trans. Electron Devices*, vol. 46, pp. 1589–1598, Aug. 1999.

[15] I. Getreu, *Modeling the Bipolar Transistor*. Beaverton, OR: Tektronix, 1976.

Guofu Niu (M'97) was born in Henan, China, in December 1971. He received the B.S. (with honors), M.S., and Ph.D. degrees in electrical engineering, all from Fudan University, Shanghai, China, in 1992, 1994, and 1997, respectively.

From December 1995 to January 1997, he was a Research Assistant at the City University of Hong Kong, and worked on mixed-level device/circuit simulation and quantum effect programmable logic gates. From May 1997 to May 2000, he conducted post-doctoral research that focused on SiGe RF devices at Auburn University, Auburn, AL. He joined the faculty in June 2000, and is currently Associate Professor of electrical and computer engineering. His research interests include SiGe devices and circuits, noise, radiation effects, SiC devices, low temperature electronics, and TCAD. He has published more than 30 journal papers and more than 20 conference papers related to his research.

Dr. Niu served on the Program Committee of the Asia–South-Pacific Design Automation Conference (ASP-DAC) in 1997, and served as a Technical Reviewer for IEEE ELECTRON DEVICE LETTERS, IEEE TRANSACTIONS ON ELECTRON DEVICES, IEEE JOURNAL OF SOLID-STATE CIRCUITS, and IEEE MICROWAVE AND GUIDED WAVE LETTERS.

John D. Cressler (F'01) received the B.S. degree in physics from the Georgia Institute of Technology, Atlanta, in 1984, and the M.S. and Ph.D. degrees in applied physics from Columbia University, New York, NY, in 1987 and 1990, respectively.

From 1984 to 1992 he was on the Research Staff, IBM Thomas J. Watson Research Center, Yorktown Heights, NY, working on high-speed Si and SiGe bipolar technology. In 1992, he left the IBM Research Division to join the faculty of Auburn University, Auburn, AL. He is currently Philpott–Westpoint Stevens Distinguished Professor of electrical and computer engineering and Director of the Alabama Microelectronics Science and Technology Center, a multidisciplinary, state-funded research center. His research interests include SiGe HBT and FET device physics, radiation effects, noise, linearity, cryogenic electronics, SiC devices and technology, Si-based RF/microwave circuits, reliability physics, device simulation, and compact circuit modeling. He has published over 220 technical papers related to his research, written four book chapters, and holds one patent. He has served as a consultant to IBM, Analog Devices, Northop–Grumman, ITRI/ERSO (Taiwan), Teltech, the National Technological University, Commercial Data Servers, MEMS-Optical, ON Semiconductor, and Texas Instruments.

Dr. Cressler received five awards from the IBM Research Division, the 1996 C. Holmes MacDonald National Outstanding Teacher Award fromEta Kappa Nu, the 1996 Auburn University Alumni Engineering Council Research Award, the 1998 Auburn University Birdsong Merit Teaching Award, the 1999 Auburn University Alumni Undergraduate Teaching Excellence Award, an IEEE Millennium Medal in 2000, and the 1994 Office of Naval Research Young Investigator Award for his SiGe research program. He is an Associate Editor for the IEEE JOURNAL OF SOLID-STATE CIRCUITS. He has served on the Technical Program Committees of the ISSCC (1992–1998, 1999–present), the BCTM (1995–1999), the IEDM (1996–1997), and the NSREC (1999–2000). He was the Technical Program Chairman of the 1998 ISSCC. He is currently Chair of the Technology Directions Subcommittee of the ISSCC, and on the Executive Steering Committee for the *MTT Topical Meeting on Silicon Monolithic Integrated Circuits in RF Systems*. He was appointed an IEEE Electron Devices Society Distinguished Lecturer in 1994.

Shiming Zhang (S'99) was born in Beijing, China, in December 1968. He received the B.E. degree in electrical engineering from Beijing Polytechnic University, Beijing, in 1992, and the M.S. degree in electrical engineering from Auburn University, Auburn, AL, in 1999, where he is currently pursuing the Ph.D. degree in electrical and computer engineering.

From 1992 to 1997, he worked on SiGe HBT at the Beijing Polytechnic University as a Research Assistant. His research interests at Beijing Polytechnic University included Layout and profiles design, dc and low temperature characterization, and fabrication processing of SiGe HBTs. His research interests include dc and microwave characterization of SiGe devices and circuits, and GaAs HBTs, broadband noise modeling of SiGe HBTs and GaAs HBTs, and radiation effects studies of SiGe HBTs and GaAs HBTs.

William E. Ansley was born in Naples, FL, on September 11, 1965. He received the B.E.E., M.S., and Ph.D. degrees in electrical engineering from Auburn University, AL, in 1991, 1994, and 1998, respectively. His dissertation work was in the area of microwave characterization and modeling of silicon–germanium heterojunction bipolar transistors.

In 1998, he joined the Microelectronics Division, IBM, East Fishkill, NY, where he is continuing to work with silicon–germanium and its applications in the personal communications market.

Charles S. Webster received the B.A. and M.S. degrees in physics from the University of Vermont, Burlington, in 1981 and 1985, respectively, and the M.S. degree in nuclear engineering sciences concentrating in radiological physics from the University of Florida, Gainesville, in 1995.

He is with IBM Microelectronics in Burlington, VT, where he specializes in RF and microwave characterization techniques in the RF/Analog Development Group.

David L. Harame (S'77–M'83–SM'01) was born in Pocatello, ID, in 1948. He received the B.A. degree in zoology from the University of California, Berkeley, in 1971, and the M.S. degree in zoology from Duke University, Durham, NC, 1973. He received the M.S. degree in electrical engineering from San Jose State University, San Jose, CA, in 1976, and the M.S. degree in materials science and the Ph.D. degree in electrical engineering, both from Stanford University, Stanford, CA, in 1984.

He joined IBM's Bipolar Technology Group at the IBM T. J. Watson Research Center, Yorktown Heights, NY, in 1984, where he worked on the fabrication and modeling of silicon-based integrated circuits. His specific research interests at Yorktown Heights included silicon and SiGe-channel FET transistors, NPN and PNP SiGe-base bipolar transistors, complementary bipolar technology, and BiCMOS technology for digital and analog and mixed-signal applications. In 1993, he joined IBM's Semiconductor Research and Development Center in the Advanced Semiconductor Technology Center, Hopewell Junction, NY, where he was responsible for the development of SiGe technology for mixed signal applications. He managed SiGe BiCMOS technology development at the ASTC through 1997. In 1998, he joined IBM's Manufacturing Organization, Essex Junction, VT, where he managed a SiGe technology group and installed the 0.5 μm SiGe BiCMOS process in the manufacturing line. In 1999, he rejoined the Semiconductor Research Corporation while remaining in Essex Junction, VT and co-managed the qualification of a 0.25 μm SiGe BiCMOS as well as 0.18 μm SIGE BiCMOS and two derivative SiGe BiCMOS technologies. In May 2000, he became the Senior Manager of the RF Analog Modeling and Design Kit Department.

Dr. Harame is a Distinguished Engineer of the IBM Corporation, an Executive Committee member of the Bipolar/BiCMOS Circuits and Technology Meeting (BCTM), and a member of the Compact Model Council.